Applied Clay Science 193 (2020) 105692

Contents lists available at ScienceDirect

Applied Clay Science

journal homepage: www.elsevier.com/locate/clay

Research Paper

Prediction of mechanical properties of grafted kaolinite – A DFT study

Eva Scholtzová[a,*], Daniel Tunega[b,c,**]

[a] Institute of Inorganic Chemistry, Slovak Academy of Sciences, Dúbravská cesta 9, SK-845 36 Bratislava, Slovak Republic
[b] Institut für Bodenforschung, Universität für Bodenkultur, Peter-Jordan-Strasse 82b, A-1190 Wien, Austria
[c] School of Pharmaceutical Science and Technology, Tianjin University, Tianjin 300072, PR China

ARTICLE INFO

Keywords:
Grafted kaolinite
Mechanical properties
Density functional theory
Dispersion corrections
Cohesion energy

ABSTRACT

Mechanical properties of kaolinite modified by grafting and/or intercalation were studied theoretically by means of the first principle calculations based on the density functional theory (DFT) method. Elastic constants, (C_{ij}), and bulk (B_0), shear (G) and Young's (E) moduli were predicted for structural models of pure kaolinite (Kaol), kaolinite intercalated with methanol (K-INT), kaolinite grafted with methoxy group (K-MTX), mixed grafted/intercalated kaolinite (K-MIX), and K-MIX model with residual water content (K-MIXW). Generally, all calculated values of the mechanical properties of the modified structures were lower than the reference values of the pure kaolinite. For example, bulk modulus decreased in a following order: 67.8 GPa (Kaol) > 41.1 GPa (K-MTX) > 34.3 GPa (K-MIXW) > 31.1 GPa (K-MIX) > 29.7 GPa (K-INT). The modification of the interlayer space by the grafting or intercalation reduced the strength of interactions between layers what was also evidenced by the calculated cohesion energies. Our calculations showed that the grafted/intercalated kaolinites represent softer materials and can be delaminated/exfoliated easier than pure kaolinite.

1. Introduction

Kaolinite ($Al_2Si_2O_5(OH)_4$) is a layered 1:1 dioctahedral aluminum silicate with layers formed by linked tetrahedral and octahedral sheets. The octahedral side of the layer is terminated by surface hydroxyl groups of μ-OH type (O atom is bound to two Al atoms). The tetrahedral side is formed by the plane of the basal surface atoms. In the kaolinite structure, layers keep together through hydrogen bonds formed among the basal oxygen atoms of the tetrahedral surface with the surface hydroxyl groups of the adjacent layer.

Kaolinite is one of the most abundant clay minerals found in the Earth's crust and has found a lot of industrial applications. This mineral can be also used as a starting material for the synthesis of new organo-mineral nanomaterials specifically designed for particular applications, for example, in environmental and remediation processes. Although the layers are held together via hydrogen bonds, kaolinite structure can expand relatively easily by intercalating various small polar molecules into the interlayer space such as potassium acetate (Wada, 1961), dimethylsulfoxide (Thompson and Cuff, 1985), *N*-methylformamide (Komori et al., 1998), methanol (Mako et al., 2015), and many others. The intercalation process opens access to basal surfaces and intercalated molecules interact usually with basal surface atoms through physical forces, mostly having hydrogen bond origin. Kaolinite intercalates can be modified by further treatment (e.g., by varying temperature and pressure) during which also chemical changes can appear (Johnston and Stone, 1990; Franco and Ruiz Cruz, 2004; Li et al., 2009). An increasing demand exists for the preparation of new hybrid materials on the kaolinite base that can be used in many industrial and environmental applications such as adsorbents, catalysts, rheological control agents, or fillers used for polymer nanocomposites, synthesis and preparation of mesoporous materials. Further, dehydroxylated kaolinite is an important part of the aluminosilicate inorganic polymers generally called geopolymers (Alzeer and MacKenzie, 2013).

The surface OH groups of the aluminol side are suitable for so-called grafting process with suitable organic agents (Tunney and Detellier, 1993; Itagaki and Kuroda, 2003; Murakami et al., 2004; Gardolinski and Lagaly, 2005; Letaief and Detellier, 2007; Avila et al., 2010; Hirsemann et al., 2011). Grafting, in general, can lead to modification of physicochemical properties of the parent material. Grafting with methanol, for example, can lead to modification of hydrophilicity/hydrophobicity of clay surfaces. Therefore, kaolinite-methanol (KM) derived structures are perspective materials applicable as precursors for obtaining kaolinite-amine derivatives and kaolinite-polymer nanocomposites (Matusik et al., 2012).

Materials prepared from kaolinite by intercalation or grafting have

* Corresponding author.
** Corresponding author at: School of Pharmaceutical Science and Technology, Tianjin University, Tianjin 300072, PR China.
E-mail addresses: eva.scholtzova@savba.sk (E. Scholtzová), daniel.tunega@boku.ac.at (D. Tunega).

https://doi.org/10.1016/j.clay.2020.105692
Received 27 March 2020; Received in revised form 20 May 2020; Accepted 20 May 2020
Available online 05 June 2020
0169-1317/

modified physical and chemical properties in comparison to the parent kaolinite mineral. Therefore, the mechanical properties can also be expected to change. Mechanical stability is one of the important factors in the preparation of kaolinite-polymer nanocomposites with desired properties. Thus, understanding and characterization of elastic properties of kaolinite-based fillers are of high importance.

Generally, it is difficult to achieve reliable and complete experimental data of elastic properties of clay minerals, mainly due to their layered structure and powder form with a grain size up to few microns. Only several experimental data for kaolinite are available in the literature. Moreover, these data show a large scattering. For example, values of bulk modulus found in the literature vary from 10 to 60 GPa (Katahara, 1996; Lonardelli et al., 2007; Mondol et al., 2008; Wenk et al., 2008). This scattering can be attributed to several factors such as origin, crystallinity and porosity of samples, size and distribution of grains, and/or the methods used in the experiment. For example, scanning and transmission electron microscopy, synchrotron X-ray diffraction, microtomography, and ultrasonic velocity measurements were used to characterize microstructures and anisotropy of the clay minerals such as kaolinite, illite-mica, and illite-smectite (Kanitpanyacharoen et al., 2011). It was found that kaolinite stacking and polytypism had only a minimal effect on the elastic properties. The Atomic Force Acoustic Microscopy (AFAM) was used to obtain elastic properties of several kaolinite clays. Young's modulus of 6.2 GPa was determined for dickite along C_{11} direction (Prasad et al., 2002). However, in another work, Young's moduli of kaolinite were determined for parallel (E_r) and perpendicular (E_z) directions to layers using nanoindentation (114 and 117 GPa) and ultrasonic echography methods (98.4 and 93.3 GPa) (Boussois et al., 2013), strongly differing from the results by Prasad et al. (2002).

Molecular modeling methods represent an effective tool for predicting various properties of kaolinite. For example, the orientation of inner hydroxyl groups in the kaolinite structure (Benco et al., 2001b), hydrogen bonds in kaolinite (Benco et al., 2001c), and potential adsorption sites at kaolinite basal surfaces (Benco et al., 2001a; Tunega et al., 2002a; Tunega et al., 2002b) were studied by means of DFT method. Further, intercalation processes of dimethylsulfoxide, −dimethylselenooxide, and *N*-methylformamide were studied by DFT, as well (Michalkova and Tunega, 2007; Scholtzová et al., 2008; Scholtzová and Smrčok, 2009; Smrčok et al., 2010a; Smrčok et al., 2010b), and calculated vibrational spectra were used in the interpretation of experimental data. The importance of the inclusion of dispersion corrections to typical DFT functionals (e.g., PBE) was shown in the systematic study of the structural parameters of four layered clay minerals, in which dispersion forces and hydrogen bonds play a dominant role in the layer stacking (Tunega et al., 2012). The ice nucleation on the hydroxylated (001) face of kaolinite via the formation of the hexagonal ice polytype was revealed by classical molecular dynamics simulations (Sosso et al., 2016). The behavior of the surface hydroxyl groups of exfoliated kaolinite in the gas phase and during water adsorption was modeled by using a set of DFT functionals on the cluster and periodic kaolinite models (Taborosi and Szilagyi, 2016). Recently, the stability of the kaolinite – methanol complex was studied by means of classical molecular dynamics and Monte Carlo simulations (Rutkai et al., 2016). Similar methods were used in the study of the effect of the basal spacing on CH_4 diffusion in kaolinite (Zhang et al., 2019). DFT method (PBE functional) was applied in the description of interactions between polyacrylamide and kaolinite (001) surface (Ren et al., 2020).

Molecular simulations methods represent also an effective way how to predict complete mechanical properties of clay minerals that is practically impossible from an experiment as clays mostly exist in a form of soft powders with a grain size of a few microns. In molecular simulations, perfect periodic structural models are used and predicted mechanical properties can represent limited values for “ideal” bulk structures. So far, several theoretical works provided mechanical properties for kaolinite or similar clay minerals. The bulk modulus and elastic constants of kaolinite were calculated from first principles using the DFT method in the work by (Sato et al., 2005). The full single-crystal elastic tensors of layered silicates such as muscovite, illite-smectite, kaolinite, dickite, and nacrite were also predicted by using DFT approach (Militzer et al., 2011). Molecular dynamics simulation based on empirical force-field description of interatomic interactions was used to study changes of structural and mechanical properties of kaolinite in a pressure range from 0 to 25 GPa (Benazzouz and Zaoui, 2012). Recently, the DFT method corrected for dispersion interactions (DFT-D2) was applied in the calculation of the kaolinite bulk modulus getting values of about 56 GPa at 298 K (Weck et al., 2015) using the Vinet and Birch–Murnaghan equations of state. Obtained results were in a good agreement with an experimental value of 59.7 GPa reported for well-crystallized samples (Welch and Crichton, 2010). In spite of the experimental or theoretical determination of mechanical properties of kaolinite minerals, so far, no similar works exist to organically modified kaolinite structures, either intercalated or grafted. In the present work, DFT-based calculations are used first time for a prediction of mechanical parameters of kaolinite modified by methanol. Particularly, elastic, bulk, shear, and Young's moduli were calculated for the kaolinite-methanol models used in our previous study of intercalated and grafted structures of kaolinite (Matusik et al., 2012). The obtained results were compared and interpreted with respect to the mechanical properties of the pure kaolinite structure. In addition, cohesion energies between layers and their changes with respect to the grafting were calculated as well.

2. Computational details

All calculations were performed using the Vienna Ab Initio Simulation Package, VASP (Kresse and Furthmuller, 1996), a code developed for electronic structure calculations on periodic structural models employing DFT approach. The parameterization of the local exchange-correlation function according to Perdew and Zunger (Perdew and Zunger, 1981), together with a generalized gradient approximation (GGA) for non-local corrections (Perdew et al., 1996) was used in the calculations. The Kohn-Sham equations were solved variationally in a plane-wave basis set with four *k*-point sampling of the Brillouin-zone (Monkhorst and Pack, 1976). The calculation of elastic properties requires precisely relaxed atomic positions and highly converged absolute energy and stress tensor. Therefore, the kinetic energy cut-off was set to 600 eV in the projector-augmented-wave (PAW) method (Blochl, 1994) and the geometry optimization procedure had a stopping criterion EDIFF = $0.1*10^{-6}$ eV for the total energy, and 0.005 eV/Å for the rms of a residual force. No symmetry restrictions were applied during any relaxation procedure. All atomic positions and unit cell parameters were relaxed. Elastic constants, $C_{ij,}$ were calculated according to a stress-strain approach. Bulk (B_0), shear (G), and Young's (E) moduli were calculated from C_{ij} using Voigt-Reuss-Hill average method (Hill, 1952).

Because of anisotropy of the structure of clay minerals (especially in the *c* direction) and relatively weak interactions between layers (hydrogen bonds), all DFT calculations were performed including the Tkatchenko-Scheffler's approach (PBE-TS + SCS) for the description of dispersion corrections (Tkatchenko et al., 2012). It was shown (Tunega et al., 2012) that by using this type of dispersion corrections, the lattice parameters of kaolinite are predicted more accurately than with the D2 corrections (Grimme, 2006) to the PBE functional.

The initial cell parameters and atomic positions of the pure kaolinite structure (*C*1 space group) were taken from the work by Neder (Neder et al., 1999) - $a = 5.154$ Å, $b = 8.942$ Å, $c = 7.401$ Å, $\alpha = 91.69°$, $\beta = 104.61°$, and $\gamma = 89.82°$. Four models of intercalated and grafted kaolinite-methanol (KM) structures (Fig. 1a-d) developed in our previous work (Matusik et al., 2012) were used for calculation of their mechanical properties in the present study. The KM models reflected several possible interactions of kaolinite with methanol in order to

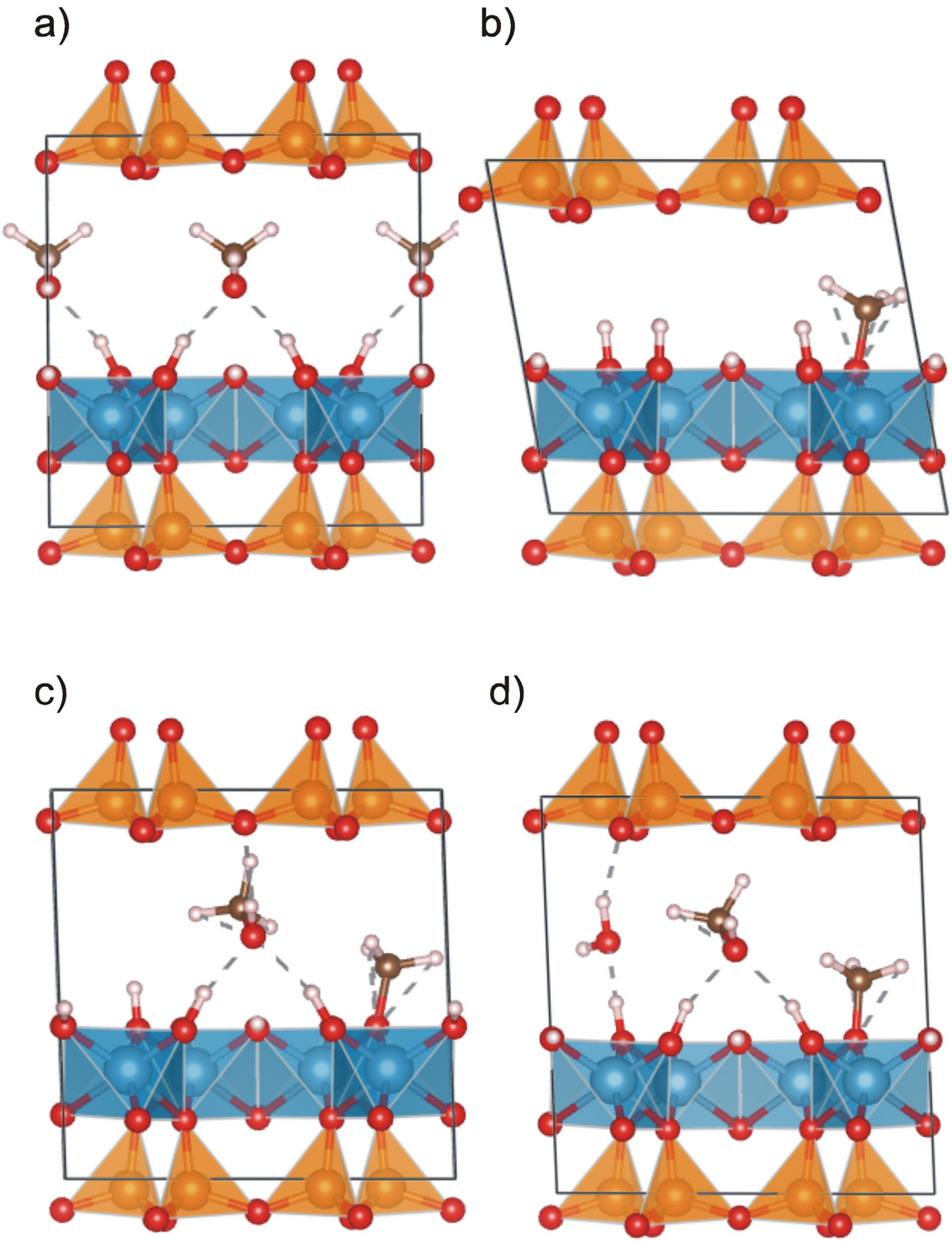

Fig. 1. Periodic structural models of modified kaolinites with methanol: a) K-INT, b) K-MTX, c) K-MIX and d) K-MIXW. Black parallelograms display unit cells.

explain experimentally determined structural parameters of methanol-modified kaolinite samples (e.g., d_{001} value).

The mechanical properties (elastic constants and moduli) were calculated for following models: i) pure kaolinite-Kaol; ii) kaolinite intercalated with two methanol molecules in the computational cell-K-INT with a summary formula $Al_4Si_4O_{10}(OH)_8(CH_3OH)_2$; iii) kaolinite grafted with one methoxy group-K-MTX. In this model, one surface OH group was substituted by one methoxy group ($Al_4Si_4O_{10}(OH)_7(CH_3O)$); iv) kaolinite intercalated with one methanol molecule and with one grafted methoxy group-K-MIX; and v) K-MIXW model, containing one additional water molecule in the computational cell of the K-MIX model. A water molecule was added to the K-MIX model because the experimental study showed that a small amount of water remains in the interlayer space after the grafting process (Matusik et al., 2012).

3. Results and discussion

3.1. Kaolinite structure

The optimized geometrical parameters (bond lengths and angles, and unit cell parameters) of the kaolinite structure calculated at the PBE-TS + SCS level of theory showed better agreement with the available experimental data (Neder et al., 1999) than those obtained at the PBE-D2 level (Matusik et al., 2012) being in the accordance with the observed trend for layered aluminosilicates in the work benchmarking several dispersion schemes (Tunega et al., 2012). It is evident,

Table 1
Optimized cell parameters [Å,°] and corresponding d_{001} value [Å] of kaolinite obtained at PBE-D2 and PBE-TS + SCS levels compared with experimental data, and optimized cell parameters and d_{001} values of kaolinite-methanol complexes (PBE-TS + SCS level).

Method/models	*a*	*b*	*c*	*α*	*β*	γ	d_{001}
PBE-D2[a]	5.173	8.982	7.314	92.0	105.2	89.8	7.15
PBE-TS + SCS	5.189	9.006	7.373	91.9	105.0	89.8	7.12
Experiment[b]	5.154	8.942	7.401	91.7	104.6	89.8	7.06
K-INT	5.177	8.938	9.876	89.9	108.0	90.0	9.39
K-MTX	5.185	8.970	9.386	80.9	120.2	90.1	7.98
K-MIX	5.220	8.993	9.450	87.9	108.1	90.0	8.98
K-MIXW	5.186	8.973	9.882	87.6	107.2	90.2	9.43

[a] Matusik et al. (2012)
[b] Neder et al. (1999)

especially for the *c* lattice constant and corresponding d_{001} value (Table 1), the most sensitive parameters with respect to the selected DFT method. For example, the d_{001} value optimized at the PBE-TS + SCS level (7.12 Å) is closer to the experimental value (7.15 Å, (Neder et al., 1999) than the value obtained with the PBE-D2 method (7.06 Å, (Matusik et al., 2012)). Table 1.

Elastic constants were calculated after the precise relaxation of the lattice parameters and atomic positions of the pure kaolinite model. These data served as reference values for comparison with calculated parameters of the models representing modified kaolinite structures. A complete matrix of the elastic constants, C_{ij}, collected in Table 2, contains twenty-one coefficients required for the full description of the total linear elasticity of triclinic crystals (Nye, 1985).

Table 2 also collects results from previous calculations and available experimental data gathered from the literature. The best agreement of our results is achieved with the PBE-D2 data from the work by (Weck et al., 2015). Observed is only a discrepancy by about 20% for the C_{33} constant. The C_{33} Young's modulus is related to the direction of the layer stacking (*c* vector) and reflects the strength of hydrogen bonding between kaolinite layers. Whereas DFT methods without the inclusion of dispersion interactions (Sato et al., 2005; Militzer et al., 2011; Weck et al., 2015) provided lateral C_{11} and C_{22} values similar to our result (Table 2), the C_{33} elastic constant showed a significant difference with our PBE-TS + SCS value (107.1 GPa). This observation is directly related to the accuracy of the optimized *c* lattice constant by different DFT methods. DFT functionals without dispersion corrections (e.g., PBE) failed in a correct prediction of the *c* parameter of kaolinite giving significantly overestimated value comparing to experiment (e.g., 7.459 Å at the PBE level (Tunega et al., 2012) comparing to 7.373 Å at the PBE-TS + SCS level). The PBE-D2 method provided a shorter *c* parameter than the PBE-TS-SCS method (Table 1) meaning that the hydrogen bond forces between layers are overestimated. Consequently, the C_{33} constant by Weck et al. (Weck et al., 2015) is overestimated as well (Table 2). Classical force-field simulations of the elastic constants (Gale, 1997) overestimated the lateral C_{11} and C_{22} parameters significantly comparing to our PBE-TS-SCS results (140% for C_{11} and almost 150% for C_{22}, respectively), whereas the C_{33} parameter was only about half our value. The elastic constants (shear moduli C_{44}, C_{55} and C_{66}, and off-diagonal C_{ij}) calculated in this work are mostly in a good agreement with the previous DFT results obtained either with or without dispersion corrections (Table 2). A certain exception is a C_{44} value that differs by about 50% from PBE and PBE-D2 values by Weck et al. (2015).

The comparison of the calculated and experimental C_{ij} values is questionable for several reasons. Practically, it is impossible to obtain a complete set of elastic constants from the experiment. Moreover, some of the available data show quite a large scattering (Table 2). It can be attributed to the fact that in experiment kaolinite samples have a powder form and, depending on the origin, they can also have a different level of crystallinity. Moreover, they can contain defects, impurities, and also residual water. On the other hand, molecular modeling calculations are performed on perfect ideal bulk structural

Table 2
Calculated and experimental elastic constants,C_{ij}, (in GPa) for kaolinite.

	Calculated						Experiment		
	This work PBE-TS + SCS	VASP[a] PBE-D2	VASP[a] PBE	CASTEP[b] PBE	VASP[c] LDA	GULP[d]	Exp[e]	Exp[f]	Exp[g]
C_{11}	177.8	175.2	187.2	179 ± 9	169.1	249.1	171.5	79.3121.1,48.1	126.4
C_{22}	174.7	168.7	180.6	201 ± 3	179.7	259.2			
C_{33}	107.1	134.0	88.0	32 ± 2	81.1	52.1	52.6	72.5112.5,45.2	57.8
C_{44}	15.5	10.1	9.6	11 ± 6	17.0	12.5	14.8	25.6, 41.1,16.7	31.6
C_{55}	11.8	12.8	12.4	22 ± 1	26.6	16.0			
C_{66}	61.6	62.3	62.1	60 ± 3	57.6	66.7	66.3	41.3	53.6
C_{12}	63.5	54.1	66.4	71 ± 7	66.1	124.8	–	–	–
C_{13}	14.1	28.6	15.6	2 ± 5	15.4	14.5	27.1	24.1, 34.8, 12.9	8.5
C_{14}	−7.3	−2	−0.7	0 ± 2	−0.4	6.4			
C_{15}	2.7	−0.8	1.2	−42 ± 1	−34.0	0.1			
C_{16}	−1.2	−5.8	−6.1	−2 ± 2	−7.8	−0.9			
C_{23}	13.5	28.5	16	−3 ± 6	10.2	18.7			
C_{24}	0.2	−2.7	−0.3	−3 ± 3	−3.4	5.7			
C_{25}	3.4	−1.4	−0.1	−20 ± 1	−16.1	1.4			
C_{26}	−2.5	1.0	0.6	2 ± 2	−0.1	6.4			
C_{34}	0.9	−3.6	−1.0	0 ± 1	−2.9	1.6			
C_{35}	−0.6	−2.4	−0.6	2 ± 2	6.7	−4.2			
C_{36}	−5.8	0.7	0.4	3 ± 2	−0.1	−0.6			
C_{45}	−0.2	−0.8	−0.5	−1 ± 1	−0.7	−0.2			
C_{46}	0.2	−1.8	−1.2	−13 ± 2	−12.4	−1.0			
C_{56}	−1.7	−0.1	−0.0	1 ± 1	1.1	−1.1			

[a] Weck et al. (2015)
[b] Sato et al. (2005)
[c] Militzer et al. (2011)
[d] GULP classical results from (Benazzouz and Zaoui, 2012), Force-Field parameters taken from (Schroder et al., 1992)
[e] Katahara (1996)
[f] Lonardelli et al. (2007)
[g] Wenk et al. (2008)

models. Finally, also a selected method in the measurement can play a role. Indeed, some experiments provided values similar to the calculated data (for example, compare C_{ij} values by Katahara (Katahara, 1996), Table 2). Based on the previous analysis, the application of the DFT method for predicting the mechanical properties of new materials seems to be a very useful tool saving the time of expensive experimental measurements.

3.2. Methanol-kaolinite structures

The optimized cell parameters of four modified models of kaolinite are collected in Table 1, together with d_{001} values. A significant expansion of the modified structures comparing to pure kaolinite is evident. The observed changes in the d_{001} parameter are similar to those obtained at the PBE-D2 level in our previous work (Matusik et al., 2012).

Comparison of our calculated elastic constants and corresponding moduli of pure kaolinite with available data from literature showed that the PBE-TS + SCS method provides reasonable data for systems, in which dispersion interactions can play an important role. Four models of kaolinite modified with methanol studied in this work (Fig. 1a-d) can represent such systems. Their elastic constants calculated at the PBE-TS + SCS level are collected in Table 3. All significant C_{ij} values decrease in the case of all four KM models comparing to the pure kaolinite (Kaol in Table 3). Generally, modification by grafting or intercalation leads to a decreasing in the stiffness of the prepared materials. It means decreasing the strength of hydrogen bond interactions between kaolinite layers by extension of the interlayer space. Guess species in the interlayer space represent less polar units than the surface OH groups and the presence of the $–CH_3$ group increases hydrophobicity in the interlayer space. Although the guess species in the interlayer space can form hydrogen bonds with the kaolinite surfaces (detailed analysis of the hydrogen bonds was done in our previous paper (Matusik et al., 2012)), these hydrogen bonds are weaker than the original hydrogen bonds between the layers. Specifically, hydrogen bonds of the $–CH_3$ groups to basal surface oxygen atoms are very weak and interactions of these groups have more dispersion character.

Table 3
PBE-TS + SCS calculated elastic constants, C_{ij}, and moduli (in GPa):B_0 – bulk modulus, G – shear modulus, E – Young's modulus; *vrh* – Voigt-Reuss-Hill average from C_{ij}, ν - Poisson's ratio.

	Kaol	K-MTX	K-MIX	K-MIXW	K-INT
C_{11}	177.8	150.9	133.4	138.4	104.3
C_{22}	174.7	167.2	155.1	142.1	114.0
C_{33}	107.1	32.5	18.5	26.3	31.5
C_{44}	15.5	10.4	8.6	8.7	13.2
C_{55}	11.8	6.2	11.8	7.9	7.5
C_{66}	61.6	46.4	43.1	39	28.2
C_{12}	63.5	34.7	37.6	35.9	21.2
C_{13}	14.1	17	10.1	8.8	8.1
C_{14}	−7.3	0	−1	1.4	−4.8
C_{15}	2.7	−1.8	0.2	1.9	5.2
C_{16}	−1.2	−1.8	−3.6	−3.6	−0.1
C_{23}	13.5	18	12	8.2	7.8
C_{24}	0.2	0.8	−0.2	1.6	2.6
C_{25}	3.4	1.2	3.3	3.1	−3.2
C_{26}	−2.5	0.2	−4.7	−4.2	0.9
C_{34}	0.9	−1	1.6	0	0.4
C_{35}	−0.6	1.8	−0.3	0.9	0.0
C_{36}	−5.8	3.7	−2.2	0.9	0.7
C_{45}	−0.2	−0.9	−0.2	0	2.2
C_{46}	0.2	0.1	0.7	0.2	−0.4
C_{56}	−1.7	−1.7	1	−0.2	0.3
B_{0vrh}	67.8	41.1	31.1	34.3	29.7
G_{vrh}	36.1	22.9	16.1	20.0	19.9
E_{vrh}	91.6	58.0	49.1	50.3	48.8
ν	0.3	0.3	0.2	0.3	0.2

To confirm the weakening of interlayer interactions in the modified kaolinite models, we performed calculations of the cohesion energy between layers for the pure kaolinite model (Kaol) and the grafted model, K-MTX (model with the highest B_0, G, and E moduli, Table 3).

For this purpose, we extended computational cells of both models in the c direction five times and performed geometry optimization for one and two layers in the extended cells. In this way, a vacuum of about ~15–20 Å was formed between one (two) layers in the neighboring computational cells (a similar approach used by Sakuma and Suehara (Sakuma and Suehara, 2015) in the calculations of interlayer bonding energies of several layered aluminosilicates including kaolinite). The interaction energy between layers was calculated as $\Delta E_{int} = E_{2L} - 2E_{1L}$, where E_{2L} and E_{1L} are total electronic energies of two and one kaolinite layers, respectively. Then, the cohesion energy was calculated as $E_{coh} = \Delta E_{int}/2A$, where A is an area determined by a and b cell vectors. The PBE-TS + SCS calculated cohesion energy for the kaolinite was 127 mJ/m^2. This result is similar to the value of ~135 mJ/m^2 obtained at the PBE-D2 level (Sakuma and Suehara, 2015). For the grafted model (K-MTX), we obtained a value of 91 mJ/m^2 meaning a significant decrease of the interaction energy between layers. Thus, K-MTX structure is energetically less stable and can be easier exfoliated than pure kaolinite.

The decrease of the cohesion energy is in full accordance with a significant drop of the C_{33} Young's modulus from 107.1 GPa (Kaol) to 32.5 GPa (K-MTX). Generally, the C_{11}, C_{22}, and C_{33} elastic constants represent moduli for axial compression, and C_{44}, C_{55} and C_{66} represent shear moduli. From them, the C_{33} constant corresponds to the direction perpendicular to the basal surface of the kaolinite layer. Surprisingly, also lateral Young's moduli, C_{11} and C_{22}, decrease for the modified KM models comparing to kaolinite. The largest decrease of the C_{11} and C_{22} coefficients is observed for the intercalated model (K-INT, Table 3) but a significant drop is also observed for two mixed models (K-MIX and K-MIXW, respectively). This observation indicates that hydrogen bonds between layers contribute to toughness in the lateral dimensions and overall structural stability of the pure kaolinite. The modification of the interlayer space either by grafting or intercalation increases the flexibility of the modified structures also in the a and b directions. Moreover, we also observed that the C_{11}/C_{22} ratio changed in all modified models (< 1) comparing to kaolinite (> 1).

As expected, the structures are the most readily deformed along c axis (reflected by the C_{33} value). According to our calculations, the highest compressibility in the c direction has the K-MIX model (18.5 GPa) and K-MIXW model (26.3 GPa) in comparison with the rest of the modified models (~ 30 GPa).

Also, the shear moduli (C_{44}, C_{55} and C_{66}) of the modified models exhibit a decrease in comparison with kaolinite. The C_{44} constant decreased by 15% for K-INT, 33% for K-MTX, 45% for K-MIX, and 44% for K-MIXW models comparing to pure kaolinite. Two other shear moduli, C_{44} and C_{55}, can also contribute to better delamination of modified kaolinite structures. The C_{55} constant decreased by 33% for K-MIXW, 36% for K-INT, and 47% for K-MTX models. Only for the K-MIX model, the C_{55} value is practically identical with the value of the pure kaolinite structure. The C_{66} shear modulus decreased by about 25% for K-MTX, 30% for K-MIX, 37% for K-MIXW, and the most for K-INT (54.2%). Lower values of C_{44} indicate lower critical resolved shear stresses, which means a better delamination process (Gardos, 1990). The delamination/exfoliation process is very important, for example, in the preparation of polymer-clay nanocomposites.

The bulk (B_0), shear (G), and Young's (E) moduli presented in Table 3 were calculated from elastic constants according to Hill. Suffix "*vrh*" of the calculated moduli denotes values calculated using Voight, Reuss and Hill approximations (Hill, 1952). It is clear that the largest values were achieved for the pure kaolinite model, whereas for all modified models the moduli were lower. From them, the grafted model (K-MTX) had bulk, shear, and Young's moduli of 41.1, 22.9, and 58 GPa, respectively. The moduli of the rest models were lower achieving

similar values ($B_0 \sim 30$ GPa, $G \sim 20$ GPa, and $E \sim 50$ GPa, Table 3).

For the K-MTX and KMIXW models, Poisson's ratio, as a ratio of transverse contraction strain to longitudinal extension strain in a direction of the stretching force, stayed similar to the kaolinite result (0.3) or decreased for the K-MIX and K-INT models (0.2). Poisson's ratio decrease can be explained by more anisotropic structures of the respective models (Greaves et al., 2011).

4. Conclusions

The DFT-based calculations performed at the PBE-TS + SCS level of theory were used in the prediction of the mechanical properties of methanol-modified kaolinite. Mechanical properties such as elastic constants and corresponding moduli were calculated for the structural models of the modified kaolinite and compared with properties of the pure kaolinite structure. In addition, cohesion energies between layers were calculated and compared as well.

Intercalation and/or grafting processes have a significant impact on mechanical parameters of all modified kaolinite structures. We observed a decrease of all calculated elastic constants and moduli including lateral C_{11} and C_{22} parameters. The most sensitive parameter (the largest decrease) is the C_{33} elastic constant that reflects a compression in a direction perpendicular to the kaolinite layers. This conclusion is in a full agreement with the calculated cohesion energies between the layers. In other words, this parameter is directly related to the type and the strength of binding between layers. Significantly lower cohesion energy was calculated for the grafted kaolinite model in a comparison with the pure kaolinite model. Lowering of the C_{44} constant of the grafted/intercalated models indicates better delamination of the modified kaolinites.

Generally, new materials prepared by grafting (intercalating) of kaolinite with small organic precursors have lowered stiffness in comparison to pure kaolinite. The selection of the proper precursor and control of the grafting (intercalation) process can lead to materials with desired properties being suitable, for example, in the preparation of clay-polymer nanocomposites. It was shown that using molecular simulation methods based on DFT theory it is possible to predict and explain various properties of clays and chemically modified clay materials (including mechanical parameters) at a good level of accuracy, which is sometimes experimentally very demanding or even impossible.

Funding

This work was supported by the Scientific Grant Agency VEGA (Grant 2/0021/19), Slovak Research and Development Agency (APVV-18-0075) and FWF-DFG project No. I3263-N34.

Declaration of Competing Interest

The authors declare that they have no known competing financial interests or personal relationships that could have appeared to influence the work reported in this paper.

Acknowledgements

ES is grateful for the financial support by the Scientific Grant Agency VEGA (Grant 2/0021/19 and Slovak Research and Development Agency (APVV-18-0075). DT acknowledges the support by the bilateral FWF-DFG project No. I3263-N34. The computational results presented have been achieved using the Vienna Scientific Cluster (VSC), project No. 70544, and using the supercomputing infrastructure of the Computing Centre of the Slovak Academy of Sciences acquired in the projects ITMS 26230120002 and 26210120002 (Slovak infrastructure for high-performance computing) supported by the Research & Development Operational Program funded by the European Regional Development Fund (ERDF).

References

Alzeer, M., MacKenzie, K., 2013. Synthesis and mechanical properties of novel composites of inorganic polymers (geopolymers) with unidirectional natural flax fibres (phormium tenax). Appl. Clay Sci. 75-76, 148–152.
Avila, L.R., de Faria, E.H., Ciuffi, K.J., Nassar, E.J., Calefi, P.S., Vicente, M.A., Trujillano, R., 2010. New synthesis strategies for effective functionalization of kaolinite and saponite with silylating agents. J. Colloid Interface Sci. 341, 186–193.
Benazzouz, B.K., Zaoui, A., 2012. A nanoscale simulation study of the elastic behaviour in kaolinite clay under pressure. Mater. Chem. Phys. 132, 880–888.
Benco, L., Tunega, D., Hafner, J., Lischka, H., 2001a. Ab initio density functional theory applied to the structure and proton dynamics of clays. Chem. Phys. Lett. 333, 479–484.
Benco, L., Tunega, D., Hafner, J., Lischka, H., 2001b. Orientation of OH groups in kaolinite and dickite: Ab initio molecular dynamics study. Am. Mineral. 86, 1057–1065.
Benco, L., Tunega, D., Hafner, J., Lischka, H., 2001c. Upper limit of the O-H center dot center dot center dot O hydrogen bond. Ab initio study of the kaolinite structure. J. Phys. Chem. B 105, 10812–10817.
Blochl, P.E., 1994. Projector augmented-wave method. Phys. Rev. B 50, 17953–17979.
Boussois, K., Deniel, S., Tessier-Doyen, N., Chateigner, D., Dublanche-Tixier, C., Blanchart, P., 2013. Characterization of textured ceramics containing mullite from phyllosilicates. Ceram. Int. 39, 5327–5333.
Franco, F., Ruiz Cruz, M.D., 2004. Factors influencing the intercalation degree ('reactivity') of kaolin minerals with potassium acetate, formamide, dimethylsulphoxide and hydrazine. Clay Miner. 39, 193–205.
Gale, J.D., 1997. GULP: a computer program for the symmetry-adapted simulation of solids. J. Chem. Soc. Faraday Trans. 93, 629–637.
Gardolinski, J., Lagaly, G., 2005. Grafted organic derivatives of kaolinite: I. Synthesis, chemical and rheological characterization. Clay Miner. 40, 537–546.
Gardos, M.N., 1990. On the elastic constants of thin solid lubricant films, in mechanics of coatings. In: Dowson, By D., Taylor, C.M., Godet, M. (Eds.), Proceedings of the 16th Leeds-Lyon Symposium on Tribology held at The Institut National des Sciences Appliquées. Elsevier Science Ltd, pp. 3–13.
Greaves, G.N., Greer, A.L., Lakes, R.S., Rouxel, T., 2011. Poisson's ratio and modern materials. Nat. Mater. 10 (vol 10, pg 823, 2011).
Grimme, S., 2006. Semiempirical GGA-type density functional constructed with a long-range dispersion correction. J. Comput. Chem. 27, 1787–1799.
Hill, R., 1952. The elastic behaviour of a crystalline aggregate. Proc. Phys. Soc. Lond. 65A, 349–354.
Hirsemann, D., Koester, T.K.J., Wack, J., van Wuellen, L., Breu, J., Senker, J., 2011. Covalent grafting to mu-hydroxy-capped surfaces? a kaolinite case study. Chem. Mater. 23, 3152–3158.
Itagaki, T., Kuroda, K., 2003. Organic modification of the interlayer surface of kaolinite with propanediols by transesterification. J. Mater. Chem. 13, 1064–1068.
Johnston, C.T., Stone, D.A., 1990. Influence of hydrazine on the vibrational-modes of kaolinite. Clay Clay Miner. 38, 121–128.
Kanitpanyacharoen, W., Wenk, H.-R., Kets, F., Lehr, C., Wirth, R., 2011. Texture and anisotropy analysis of Qusaiba shales. Geophys. Prospect. 59, 536–556.
Katahara, K.W., 1996. Clay mineral elastic properties. In: 66th Annual International meeting, SEG Expanded Abstracts, pp. 1691–1694.
Komori, Y., Sugahara, Y., Kuroda, K., 1998. A kaolinite-NMF-methanol intercalation compound as a versatile intermediate for further intercalation reaction of kaolinite. J. Mater. Res. 13, 930–934.
Kresse, G., Furthmuller, J., 1996. Efficient iterative schemes for ab initio total-energy calculations using a plane-wave basis set. Phys. Rev. B 54, 11169–11186.
Letaief, S., Detellier, C., 2007. Functionalized nanohybrid materials obtained from the interlayer grafting of aminoalcohols on kaolinite. Chem. Commun. 2613–2615.
Li, Y., Sun, D., Pan, X., Zhang, B., 2009. Kaolinite intercalation precursors. Clay Clay Miner. 57, 779–786.
Lonardelli, I., Wenk, H.-R., Ren, Y., 2007. Preferred orientation and elastic anisotropy in shales. Geophysics 72, D33–D40.
Mako, E., Kovacs, A., Hato, Z., Kristof, T., 2015. Simulation assisted characterization of kaolinite-methanol intercalation complexes synthesized using cost-efficient homogenization method. Appl. Surf. Sci. 357, 626–634.
Matusik, J., Scholtzová, E., Tunega, D., 2012. Influence of synthesis conditions on the formation of a kaolinite-methanol complex and simulation of its vibrational spectra. Clay Clay Miner. 60, 227–239.
Michalkova, A., Tunega, D., 2007. Kaolinite : dimethylsulfoxide intercalatea theoretical study. J. Phys. Chem. C 111, 11259–11266.
Militzer, B., Wenk, H.R., Stackhouse, S., Stixrude, L., 2011. First-principles calculation of the elastic moduli of sheet silicates and their application to shale anisotropy. Am. Mineral. 96, 125–137.
Mondol, N.H., Jahren, J., Brevik, I., 2008. Elastic properties of clay minerals. Lead. Edge 27, 758–770.
Monkhorst, H.J., Pack, J.D., 1976. Special points for Brillouin-zone integrations. Phys. Rev. B 13, 5188–5192.
Murakami, J., Itagaki, T., Kuroda, K., 2004. Synthesis of kaolinite-organic nanohybrids with butanediols. Solid State Ionics 172, 279–282.
Neder, R.B., Burghammer, M., Grasl, T., Schulz, H., Bram, A., Fiedler, S., 1999. Refinement of the kaolinite structure from single-crystal synchrotron data. Clay Clay Miner. 47, 487–494.
Nye, J.F., 1985. Physical Properties of Minerals. Clarendon Press, Oxford, UK.
Perdew, J.P., Zunger, A., 1981. Self-interaction correction to density-functional

approximations for many-electron systems. Phys. Rev. B 23, 5048–5079.
Perdew, J.P., Burke, K., Wang, Y., 1996. Generalized gradient approximation for the exchange-correlation hole of a many-electron system. Phys. Rev. B 54, 16533–16539.
Prasad, M., Kopycinska, M., Rabe, U., Arnold, W., 2002. Measurement of Young's modulus of clay minerals using atomic force acoustic microscopy. Geophys. Res. Lett. 29.
Ren, B., Min, F.F., Liu, L.Y., Chen, J., Liu, C.F., Lv, K., 2020. Adsorption of different PAM structural units on kaolinite (001) surface: density functional theory study. Appl. Surf. Sci. 504.
Rutkai, G., Hato, Z., Kristof, T., 2016. Stability of the kaolinite-guest molecule intercalation system: a molecular simulation study. Fluid Phase Equilib. 409, 434–438.
Sakuma, H., Suehara, S., 2015. Interlayer bonding energy of layered minerals: Implication for the relationship with friction coefficient. J. Geophys. Res. Solid Earth 120, 2212–2219.
Sato, H., Ono, K., Johnston, C.T., Yamagishi, A., 2005. First-principles studies on the elastic constants of a 1 : 1 layered kaolinite mineral. Am. Mineral. 90, 1824–1826.
Scholtzová, E., Smrčok, Ľ., 2009. Hydrogen bonding and vibrational spectra in kaolinite-dimethylsulfoxide and -dimethylselenoxide intercalates–a solid-state computational study. Clay Clay Miner. 57, 54–71.
Scholtzová, E., Benco, L., Tunega, D., 2008. A model study of dickite intercalated with formamide and N-methylformamide. Phys. Chem. Miner. 35, 299–309.
Schroder, K.P., Sauer, J., Leslie, M., Catlow, C.R.A., Thomas, J.M., 1992. Bridging hydroxyl-groups in zeolitic catalysts - a computer-simulation of their structure, vibrational properties and acidity in protonated faujasites (H-Y zeolites). Chem. Phys. Lett. 188, 320–325.
Smrčok, Ľ., Tunega, D., Ramirez-Cuesta, A.J., Ivanov, A., Valúchová, J., 2010a. The combined inelastic neutron scattering (ins) and solid-state dft study of hydrogen-atoms dynamics in kaolinite-dimethylsulfoxide intercalate. Clay Clay Miner. 58, 52–61.
Smrčok, Ľ., Tunega, D., Ramirez-Cuesta, A.J., Scholtzová, E., 2010b. The combined inelastic neutron scattering and solid state DFT study of hydrogen atoms dynamics in a highly ordered kaolinite. Phys. Chem. Miner. 37, 571–579.
Sosso, G.C., Tribello, G.A., Zen, A., Pedevilla, P., Michaelides, A., 2016. Ice formation on kaolinite: Insights from molecular dynamics simulations. J. Chem. Phys. 145.
Taborosi, A., Szilagyi, R.K., 2016. Behaviour of the surface hydroxide groups of exfoliated kaolinite in the gas phase and during water adsorption. Dalton Trans. 45, 2523–2535.
Thompson, J.G., Cuff, C., 1985. Crystal-structure of kaolinite - dimethylsulfoxide intercalate. Clay Clay Miner. 33, 490–500.
Tkatchenko, A., DiStasio, R.A., Car, R., Scheffler, M., 2012. Accurate and efficient method for many-body van der waals interactions. Phys. Rev. Lett. 108.
Tunega, D., Benco, L., Haberhauer, G., Gerzabek, M.H., Lischka, H., 2002a. Ab initio molecular dynamics study of adsorption sites on the (001) surfaces of 1 : 1 dioctahedral clay minerals. J. Phys. Chem. B 106, 11515–11525.
Tunega, D., Haberhauer, G., Gerzabek, M.H., Lischka, H., 2002b. Theoretical study of adsorption sites on the (001) surfaces of 1 : 1 clay minerals. Langmuir 18, 139–147.
Tunega, D., Bucko, T., Zaoui, A., 2012. Assessment of ten DFT methods in predicting structures of sheet silicates: importance of dispersion corrections. J. Chem. Phys. 137.
Tunney, J.J., Detellier, C., 1993. Interlamellar covalent grafting of organic units on kaolinite. Chem. Mater. 5, 747–748.
Wada, K., 1961. Lattice expansion of kaolin minerals by treatment with potassium acetate. Am. Mineral. 46, 78–91.
Weck, P.F., Kim, E., Jove-Colon, C.F., 2015. Relationship between crystal structure and thermo-mechanical properties of kaolinite clay: beyond standard density functional theory. Dalton Trans. 44, 12550–12560.
Welch, M.D., Crichton, W.A., 2010. Pressure-induced transformations in kaolinite. Am. Mineral. 95, 651–654.
Wenk, H.R., Voltolini, M., Mazurek, M., Van Loon, L.R., Vinsot, A., 2008. Preferred orientations and anisotropy in shales: Callovo-Oxfordian shale (France) and opalinus clay (Switzerland). Clay Clay Miner. 56, 285–306.
Zhang, B., Kai, W., Kang, T.H., Kang, G.X., Zhao, G.F., 2019. Effect of the basal spacing on CH4 diffusion in kaolinite. Chem. Phys. Lett. 732.